

Localization of quantum particles with long-range hopping in 3D lattices of finite size

J. T. Cantin, T. Xu, and R. V. Krens

Department of Chemistry, University of British Columbia, Vancouver, B.C., V6T 1Z1, Canada

(Dated: February 15, 2017)

Non-interacting particles with long-range hopping are known to be delocalized in disordered systems of infinite size. It is thus natural to assume that such particles can traverse any finite-size lattice. Here, we demonstrate that this is not generally true. The delocalization mechanism is induced by resonances between distant lattice sites. The number of such resonances diverges with the system size. For a finite-size lattice the number of resonances is finite and may not be sufficient to result in delocalization. We consider particles with long-range (dipolar) hopping in three-dimensional lattices with diagonal disorder and random dilution. We compute the wavepacket dynamics of particles placed in an individual lattice site, the inverse participation ratios and the fluctuations of the wavefunctions with disorder. We show that, for certain finite-size disordered lattices, particles remain localized within a finite volume much smaller than the lattice size, and that the wavefunctions exhibit the log-normal fluctuations characteristic of Anderson localization. We characterize the localization properties as functions of dilution and diagonal disorder. We combine our results with scaling theory to obtain the size dependence of the localization–diffusion crossover. Our results indicate that particles with long-range hopping undergo exponential localization in lattices of finite size, even macroscopically finite. Our phase diagrams illustrate a rather unusual phenomenon: quantum particles can diffuse through a lattice of size $10A$, but not through a lattice of size A .

INTRODUCTION

A quantum particle in a three-dimensional disordered lattice is either localized or diffusive; this depends on the strength of the disorder [1]. If the particles are localized within a finite localization length λ , one observes current over length scales $\lesssim \lambda$, while no conductivity over length scales $\gg \lambda$ [2]. If quantum transport is allowed over infinite length scales, particles are naturally assumed to diffuse over any arbitrary length scale. As was pointed out already in the original work of Anderson [3], quantum particles with long-range hopping are diffusive in three-dimensional (3D) lattices of infinite size, for any disorder strength. This absence of localization was later explained by Levitov [4–7], who showed that diffusion occurs due to resonant transitions between distant lattice sites. The number of such resonances diverges with the lattice size, leading to particle transport over infinite length scales. However, if the lattice size is finite, the number of resonances is also finite. This raises the question: If the lattice size is reduced, can the system localize to length scales smaller than the lattice size or will the localization length always remain larger than the system size?

To answer this question, we consider particles with dipolar hopping in 3D disordered lattices. Dipolar hopping is long-range in 3D. For generality, we consider lattices with random on-site energies and random dilution. We show that as the lattice size is *reduced*, delocalized particles may, depending on the dilution and amount of disorder, become localized to length scales much smaller than the lattice size. This leads to a rather unusual phenomenon: particles can diffuse through a lattice of size $10A$, but not through a lattice of size A . This means that quantum currents can be switched off by shrinking the size of the system.

For conventional disordered systems, the localization is typically characterized by computing certain properties as functions of the lattice size. For example, one can examine the distribution of nearest spacings of the Hamiltonian eigenvalues, which must undergo a change from the Wigner distribution to a Poisson distribution near the diffusion–localization crossover. This change becomes sharper as the lattice size increases, corresponding to a phase transition in the infinite size limit. For particles with dipolar long-range hopping in 3D lattices, such conventional analyses are not possible as the parameters of interest are functions of the system size itself and the localization length diverges with the system size, in contrast to the case with nearest neighbour hopping. Therefore, in order to examine the properties of particles with long-range hopping in finite-size lattices, we use the following approach:

- (i) First, we compute the wavepacket expansion dynamics of particles placed in an individual site of the lattice to show that, for certain system parameters, a particle placed in the middle of the lattice does not reach the lattice edge over long times greatly exceeding the Heisenberg time;
- (ii) Second, we compute the inverse participation ratio for each eigenstate of the Hamiltonian to illustrate that, for certain system parameters, all eigenstates are localized to parts of the lattice much smaller than the lattice size;
- (iii) Third, we examine the fluctuations of the wavefunctions between instances of disorder to illustrate that these fluctuations become log-normal at strong disorder;

- (iv) Fourth, we map out the localization-diffusion crossover region as a function of dilution and on-site disorder using the wavepacket dynamics described in (i);
- (v) Finally, we combine our results with scaling theory from Refs. [4–7] in order to obtain the dependence of the localization - diffusion crossover region on the lattice size. Refs. [4–7] were originally introduced to explain delocalization of particles with long-range hopping.

WAVEPACKET DYNAMICS

We consider particles with dipolar hopping in 3D disordered lattices, known to be diffusive over infinite length scales. We start by illustrating the absence of diffusion for such particles in finite-size lattices by computing the time evolution of wavepackets placed on an individual lattice site. For generality, we compute the wavepacket dynamics in a diluted, disordered lattice and characterize the localization-diffusion phase diagram as a function of both dilution and disorder strength, as was done for particles with short-range hopping in Ref. [2].

The dynamics are governed by the following Hamiltonian:

$$\hat{H} = \sum_i w_i \hat{c}_i^\dagger \hat{c}_i + \sum_i \sum_{j \neq i} t_{ij} \hat{c}_i^\dagger \hat{c}_j, \quad (1)$$

where the operator \hat{c}_i removes the particle from site i , w_i is the energy of the particle in site i , and t_{ij} is the amplitude for particle tunnelling from site j to site i . We introduce disorder by randomizing both the values of w_i and t_{ij} , which makes Eq. (1) relevant for both disordered lattices and amorphous systems.

We consider a single particle in a 3D cubic lattice with N sites per dimension. We randomize the values $w_i \in [-w/2, w/2]$ drawn from a uniform distribution and the values t_{ij} as in the site percolation model. For a given realization of disorder, we divide the lattice sites into two subsets P and Q , with pN^3 sites in the P subset and $(1-p)N^3$ in the Q subset. For a given value p , the lattice sites are assigned to the subsets at random. The hopping amplitudes of the Hamiltonian (1) are then defined as follows:

$$t_{ij} = \begin{cases} \frac{\gamma}{|\mathbf{r}_{ij}|^\alpha}, & i \in P \text{ and } j \in P \\ 0, & i \in Q \text{ and/or } j \in Q \end{cases} \quad (2)$$

where $\mathbf{r}_{ij} = \mathbf{r}_i - \mathbf{r}_j$ is the distance between sites i and j and α determines the hopping range, with $\alpha = 3$ representing dipolar hopping. The value of γ is chosen such that $t_{ij} \equiv \tilde{t} = 1$ for nearest neighbour (NN) sites. With t_{ij} thus defined, the Hamiltonian (1) describes a particle with dipolar hopping in a disordered, diluted lattice with

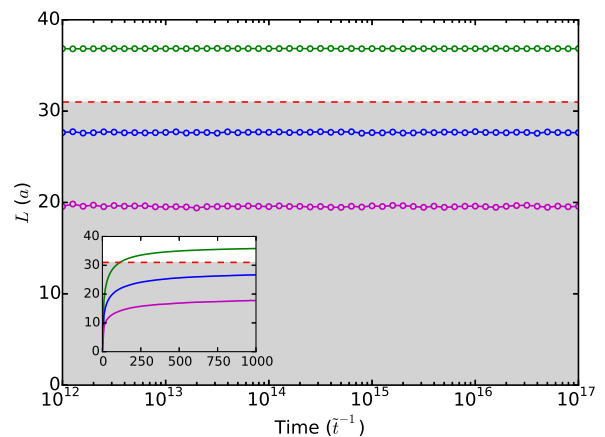


FIG. 1. Time-dependence of the wavepacket size L for a particle initially at the centre site. L is the diameter of a sphere containing no less than 90% of the particle density. The particle has $t_{ij} \propto |\mathbf{r}_{ij}|^{-3}$ and is in a disordered lattice with $N^3 = 31^3$, $p = 0.5$ and $w = 5, 10$, and 20 (green, blue, and magenta, respectively). The horizontal dashed line shows the side-length of the cubic lattice; the grey area highlights sizes smaller than this. The inset shows the same observables, but over shorter time scales. The values of L are averaged over 1050 realizations of disorder. The Heisenberg time for these systems is $\sim 300 \tilde{t}^{-1}$, as can also be seen from the inset.

pN^3 sites. The system parameters of interest are p , w , and N .

We compute the wavepacket dynamics for a particle placed at the center of the cubic lattice. As described in Ref. [8], we use the eigenstates of the Hamiltonian (1) to construct the time propagator and compute the wavefunction of the particle at extremely long times $> 10^{17} \tilde{t}^{-1}$, far exceeding the Heisenberg time (typically $\sim 300 \tilde{t}^{-1}$ for the systems considered here). To characterize the spread of the wavepacket in real space, we compute the diameter L of the sphere enclosing at least 90% of the particle density as a function of time. The values of L are averaged over 200 to 1050 realizations of disorder, as required for convergence and as specified in the figure captions. Figure 1 shows the dependence of L on time for $p = 0.5$ and for different values of w . As expected, for systems with low values of w , the particle density expands to fill the entire lattice. However, for lattices with $w = 10$ and $w = 20$, the particle density, on average, does not reach the lattice size and remains localized on a scale smaller than the lattice size.

INVERSE PARTICIPATION RATIOS

The results of Figure 1 illustrate that lattices with large w do not permit diffusion of particles with dipolar hopping over long time scales. The slopes of the curves

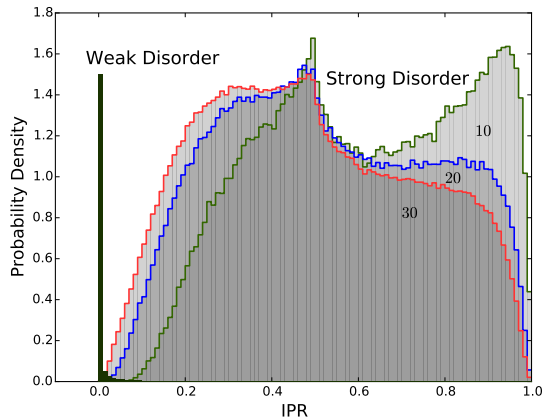


FIG. 2. The distributions of the inverse participation ratios of the eigenstates of the Hamiltonian (1) computed for a point with strong disorder ($w = 17.5$; $p = 0.18$) and a point with weak disorder ($w = 4$; $p = 0.8$; $N^3 = 30^3$). The IPR distributions for the point with strong disorder are computed for three lattice sizes with $N^3 = 10^3$, 20^3 and 30^3 , illustrating a slow shift towards the diffusion regime recovered in the infinite size limit (see Figure 5). The distributions are averaged over 1300 ($N^3 = 10^3$) and 300 ($N^3 = 20^3$ and $N^3 = 30^3$) instances of disorder.

in Figure 1 are zero (within the numerical uncertainties), which indicates the absence of diffusion over infinite time. However, a numerical calculation of wavepacket dynamics cannot strictly prove the absence of diffusion at infinite time. In order to confirm localization and gain a better understanding of the eigenstates of the system, we compute the inverse participation ratio (IPR) distribution of the entire set of the eigenstates of the Hamiltonian (1) for two different dilutions and disorder strengths and at different system sizes.

Figure 2 shows these IPR distributions for a point with weak disorder ($w = 4$; $p = 0.8$; $N^3 = 30^3$) and strong disorder ($w = 17.5$; $p = 0.18$; $N^3 = 10^3, 20^3, 30^3$). For states delocalized over the entire lattice, the IPR tends to $(pN^3)^{-1}$. For states localized on a single lattice site, the IPR is one. Figure 2 shows that for weak disorder the IPR is narrowly distributed near zero, meaning that nearly all of the eigenstates are delocalized over most of the lattice. The IPR for strong disorder is markedly different, with all states having a much higher IPR.

To identify the point with strong disorder as in a localized regime, it is important to prove that the distributions have absolutely no states with the IPR close to $I_d = (pN^3)^{-1}$. To do this, we analyzed the distributions in Figure 2 for each instance of disorder separately, to compute the minimum value of the IPR, I_{\min} , which represents the *most extended* eigenstate. We obtained the following results: of 1300 disorders for $N^3 = 10^3$, the smallest ratio $I_{\min}/I_d = 10.6$; of 300 disorders for

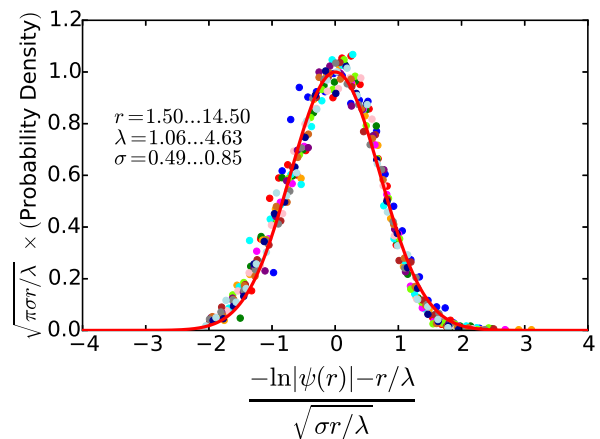


FIG. 3. Scaled histogram of $\ln |\psi(r)|$ for $N^3 = 31^3$, $p = 0.5$, $w = 80$ computed at time $T = 10^{17}t^{-1}$. The different colours refer to histograms at different values of r . The values of λ and σ are obtained by scaling the computed histograms using the formula shown on the abscissa. λ corresponds to the localization length. The red curve shows e^{-x^2} , with x the abscissa. The results are obtained using 3150 realizations of disorder.

$N^3 = 20^3$, $I_{\min}/I_d = 25.0$; of 300 disorders for $N^3 = 30^3$, $I_{\min}/I_d = 20.1$. This means that the *most extended* eigenstate of many disorder realizations is confined to less than one tenth of all lattice sites, proving that all eigenstates are confined to a volume much smaller than the lattice size. For comparison, the same ratio for the diffusive regime distribution in Figure 2 is $I_{\min}/I_d = 1.7$. As the lattice size increases, the IPR distributions shift toward zero. These shifts should collapse the IPR distributions to a single line at zero in the limit of infinite size. However, Figure 2 shows that the approach of the distributions to that in the diffusive regime is very slow, suggesting that a localized regime could be expected to exist even for systems of large size.

LOG-NORMAL FLUCTUATIONS

While the results of the previous section illustrate that all eigenstates of the strongly disordered Hamiltonians are confined to a fraction of the lattice sites, the IPR values do not provide information on the shape of the wavefunctions. Here, we demonstrate that the wavefunctions are exponentially localized by computing the fluctuations of the particle density between instances of disorder. We also determine the corresponding localization length.

One of the characteristic features of Anderson localization is the log-normal distribution of the particle density across disorder realizations [9]. For example, as shown in section 2 of Ref. [10], the transmission T through a disordered region in the regime of Anderson localization

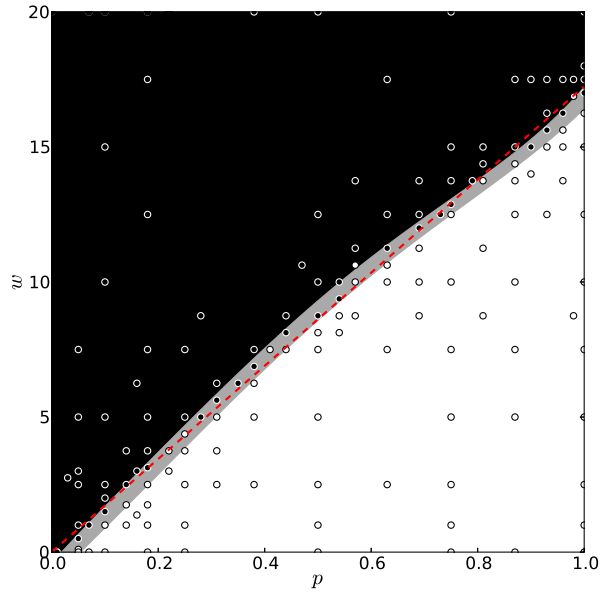


FIG. 4. The wavefunction spread L for a particle with $t_{ij} \propto |\mathbf{r}_{ij}|^{-3}$ initially placed in the middle of a 3D lattice with $N^3 = 25^3$ after $10^{17}\hat{t}^{-1}$. The circles indicate the computed values, averaged over 200 to 600 realizations of disorder, as required for convergence. For points in the black area, $L < N$, indicating the absence of transport. The white area corresponds to $L \geq N$, indicating diffusion to the lattice edges in finite time. The grey area shows the crossover regime, where some values of (w, p) allow diffusion to the lattice edges and some not. The dashed line in the lower panel is the $N^3 = 25^3$ line from Figure 5, determined as described in the text.

follows a log-normal distribution, in contrast to the diffusive case where T follows a normal distribution. In the regime of Anderson localization, $\ln T$ thus follows a normal distribution. Since $\ln T$ is proportional to the extinction coefficient K , the extinction coefficient also follows a normal distribution. The average of K over instances of disorder is R/λ (see Eqn. 21 of Ref. [10]), where R is the system length and λ is the localization length. The typical amplitude of an Anderson-localized wavefunction $|\psi|_{\text{Typ}}^2 \propto \exp(-x/\lambda)$, where x is distance. For a specific instance of disorder, an Anderson-localized wavefunction would then be $|\psi|^2 \propto \exp(-Kx/R)$. Thus, at a specific value of x , the magnitude of the wavefunction will vary log-normally between instances of disorder. This log-normal distribution is equivalent to the exponential decay of the wavefunction in real space.

We plot in Figure 3 the histograms of $\ln |\psi(r)|$ for the lattice with $N^3 = 31^3$, $p = 0.5$, and $w = 80$. $|\psi(r)|$ is obtained from wavepacket dynamics calculations at time $T = 10^{17}\hat{t}^{-1}$. The histograms for different values of r (distance from the site of maximum density) are scaled to lie on the same curve. The scaling is performed using the formula displayed on the abscissa of Figure 3. The

parameter λ corresponds to the localization length. The values obtained are displayed in Figure 3.

Figure 3 shows that these scaled histograms all follow a Gaussian distribution, illustrating the *log-normal* distribution of the particle density vs disorder realizations:

$$\mathcal{N}(\ln |\psi|, r; \sigma, \lambda) = \frac{1}{\sqrt{\pi\sigma r/\lambda}} \exp \left[-\frac{(\ln |\psi(r)| - r/\lambda)^2}{\sigma r/\lambda} \right].$$

This log-normal behaviour shows that particles with long-range hopping undergo exponential decay in finite-size systems. Exponential decay is one key feature of Anderson localization. Moreover, the data in Figure 3 show that the localization length (see λ in Figure 3) is much smaller than the side-length of the lattice ($N = 31$).

DIFFUSION-LOCALIZATION CROSSOVER

To understand the dependence of the diffusion/localization properties on the dilution and the on-site disorder, we repeat the wavepacket dynamics calculations of Figure 1 for different values of p and w . The results are presented in Figure 4.

Figure 4 shows two regimes: the black area corresponds to what would be observed in any experiment as the localization regime; the white area corresponds to the diffusive regime. To obtain these results, we first fix the lattice size and determine by a large number of computations whether a particle initially in the middle of the 3D lattice spreads to fill the entire lattice or forms a localized wavepacket that, after the long time $10^{17}\hat{t}^{-1}$, stays, on average, within a sphere of size L smaller than the lattice size.

We would like to emphasize that Figure 4 is *not* a phase diagram as phase diagrams correspond to the thermodynamic limit and the present results are for a finite-size lattice. Similarly, what we identify is a localization-diffusion *crossover*, not a localization-diffusion *transition*.

The area of Figure 4 coloured in black corresponds to disorders where the average size L of the wavepacket is smaller than the lattice size; i.e., where, on average, there is no diffusion to the lattice edges over the long time $10^{17}\hat{t}^{-1}$. We note that the absence of localization along the horizontal axis of Figure 4 is consistent with the recent work of Ref. [11] that shows no localization for a 3D system with dipolar hopping on a diluted lattice and no on-site disorder ($w = 0$). Clearly, the off-diagonal disorder caused by the diluted lattice is insufficient to cause localization; diagonal disorder is required. This also illustrates the absence of either a quantum or classical percolation threshold for a system of this size.

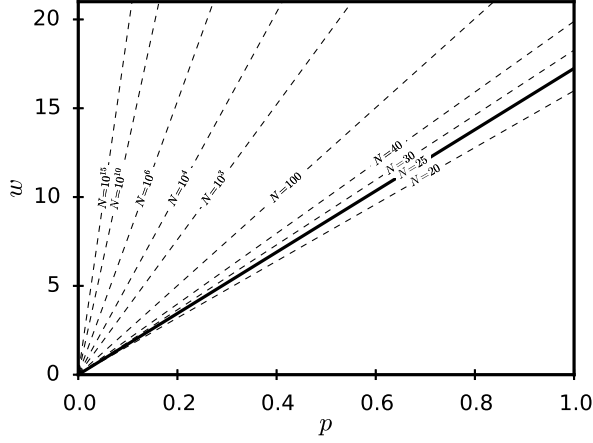


FIG. 5. Lattice-size dependence of the localization-diffusion crossover for particles in a 3D lattice with long-range tunnelling $t_{ij} \propto |\mathbf{r}_{ij}|^{-3}$. The solid line corresponds to the dashed line in Figure 4, determined as discussed in the text.

LATTICE-SIZE DEPENDENCE

It is important to analyze how Figure 4 changes with the size of the lattice. To do this, we combine the results of wavepacket calculations in Figure 4 with the scaling analysis of Levitov [7]. From Ref. [7], delocalization occurs through resonances defined by $t_{ij} \geq |w_i - w_j|$. The number of resonances diverges with the system size and delocalization must occur when

$$\frac{28\pi}{3}\kappa\lambda \gg 1, \quad (3)$$

where $\lambda = \tilde{t}p/w$ and κ is the index of a concentric sphere with radius $2^\kappa R$. Re-written as $\frac{28\pi}{3}\kappa\lambda = a$, where a is some large constant, Eq. (3) produces a line in the (p, w) -phase diagram separating the diffusive and localized regimes:

$$w = p \times \tilde{t} (A + B \ln N), \quad (4)$$

where we assumed that $2^\kappa R \propto N$ and A and B are unknown constants. To determine A and B , we first note that the probability distribution of the site energy differences is

$$P(\delta) = \frac{2}{w} \left(1 - \frac{\delta}{w}\right), \text{ where } \delta = |w_i - w_j| \in [0, w], \quad (5)$$

and calculate the probability of resonance between sites i and j as

$$P(p, \gamma, w, r_{ij}) = pP(\delta \leq t_{ij}) = \frac{2p\gamma}{wr_{ij}^3} - \frac{p\gamma^2}{w^2r_{ij}^6}. \quad (6)$$

Using Eq. (6), we calculate the probability \tilde{P} that the central site has *no* resonance in the entire system of a

given size and draw the isoprobability lines for $N^3 = 25^3$ on the diagram from Figure 4. The isoprobability line with $\tilde{P} = 1.2 \times 10^{-2}$ goes through the localization-diffusion crossover diagram inside the grey crossover regime, as shown in Figure 4. Using this value of \tilde{P} as characterizing the diffusion-localization crossover, we obtain the crossover lines for $N^3 = 21^3; 31^3; 41^3; 101^3$ and fit Eq. (4) to the resulting curves to obtain A and B . To verify the procedure, we compute the isoprobability lines for $N^3 = 301^3$ and $N^3 = 1001^3$, and obtain a perfect agreement with the values from Eq. (4). Figure 5 shows the crossover lines for different lattice sizes. Remarkably, Figure 5 illustrates that the localization crossover may occur at finite values of w for systems with a macroscopically large size. Consider, for example, the case with $N^3 = (10^8)^3$, which corresponds to a 3D lattice with 10^{24} sites, which exceeds Avogadro's number. In the infinite size limit, the crossover line tends to the y -axis, which corresponds to the absence of localization and is consistent with prior work [3–7].

EXPERIMENTAL RELEVANCE AND APPLICATIONS

Our results illustrate that the detection of the crossover for particles with dipolar hopping in 3D lattices is within reach of current experiments. This can be done with ions in rf-traps, ultracold magnetic atoms, ultracold Rydberg atoms, or ultracold molecules trapped in optical lattices. An optical lattice typically contains ≈ 60 sites per dimension. Localization can be observed with internal excitations of the trapped atoms or molecules [12–16]. If an optical lattice is partially populated with atoms or molecules, the empty lattice sites serve as impurities that scatter the excitations. The parameter p in the diagram shown in Figure 4 can thus be controlled by simply varying the number of atoms or molecules loaded in the optical lattice. The disorder in w_i can be applied using an optical speckle potential, as in [17–20]. For example, Figure 5 shows that for molecules on an optical lattice with $N \approx 60$ and a lattice population of 30 % [13], the crossover can be observed by varying the optical speckle potential from below to above $w = 5$.

Our results have, at least, three major applications. First, they can be used for the design of miniaturized quantum devices relying on the transport of small excitons that move via dipolar hopping. Our results show how much disorder can be tolerated in such devices and what is the minimum length scale of such devices that allows high exciton mobility. Second, our results show how one can engineer exciton transport on small length scales by doping molecular crystals with impurities. This is relevant for bulk heterojunction organic solar cells and similar light-harvesting devices that rely on the high mobility of excitons [22, 23]. Third, our results are crit-

ical for the design of experiments aimed at detection of interaction-induced many-body localization (MBL). MBL is predicted to hinder the return of a perturbed quantum system to equilibrium, thus precluding thermalization, conductivity, density equilibration or energy transport. It is the subject of numerous theoretical studies, many of which propose experiments for the observation of the localized phase. Of particular interest is the localization phase transition in 3D dipolar systems, where excitations/spins hop between carrier particles due to dipolar interactions. A recent startling discovery [24] shows that the localized phase can be induced by interactions between the particles. In order for such a phase transition to be observable, the system must be in the diffusive regime in the limit of non-interacting particles. Our work shows that this is not guaranteed and provides the conditions required to perform these experiments.

CONCLUSION

Particles with long-range hopping are known to be delocalized in lattices of infinite size. Here, we have presented evidence that particles with dipolar long-range hopping may undergo exponential localization in 3D disordered lattices of finite size. Our conclusions are based on three independent but mutually consistent results:

- (i) First, we have demonstrated by rigorous quantum dynamics calculations that particles placed in an individual lattice site cannot diffuse through lattices of finite size over long time scales. By itself, this is not sufficient proof of localization as this result does not rule out the possibility that particles can fill the entire lattice at infinite time.
- (ii) To further confirm the presence of localization, we have calculated the inverse participation ratio for each eigenstate of the Hamiltonian. Our results show that no eigenstate occupies more than 10 % of the lattice for lattices of sufficiently small finite size. Our results also show how the participation ratio changes with increasing system size towards a system with delocalized states. One may argue that this is not sufficient proof of localization as it does not rule out the possibility of states that occupy a small number of lattice sites that are spread throughout the lattice (for example, every tenth site). However, the presence of such states would allow for significant transport through the lattice, which we do not observe in (i).

The results in (i) and (ii) thus provide strong evidence for localization in finite-size lattices. However, the shape of the wavefunctions is still not clear. To better understand this,

- (iii) we have computed the fluctuations of the wavefunctions between instances of disorder. Our results illustrate that the wavefunction fluctuations follow a log-normal distribution, which corresponds to exponential localization of the wavefunctions.

Our results in Figure 4 illustrate the crossover between what would be observed in any experiment as the localization regime and the diffusion regime. We have demonstrated that introducing diagonal disorder can bring the system to the localization regime, even if introducing dilution alone cannot [11]. Furthermore, introducing diagonal disorder alone is sufficient to observe the localization regime. The crossover is shown to be within reach of current experiments.

We would like to emphasize that the absence of localization with dilution alone (x-axis of Figure 4) shows that there is no classical or quantum percolation threshold for a system of this size. The lack of classical localization means that any localization induced by diagonal disorder must be due to quantum interference effects.

We have combined our wavepacket calculations in Figure 4 with the scaling theory from Refs. [4–7] to demonstrate how the crossover changes with the system size (Figure 5). Surprisingly, we find that one should expect to observe the absence of quantum transport even in systems with macroscopically finite size, providing the on-site disorder and the dilution are significant enough. These results are of practical interest as they can be used to inform the design of miniaturized quantum devices, which always have finite size.

ACKNOWLEDGMENTS

We acknowledge useful discussions with Andreas Buchleitner. This work is supported by NSERC of Canada.

-
- [1] E. Abrahams, P. W. Anderson, D. C. Licciardello, and T. V. Ramakrishnan, *Phys. Rev. Lett.* **42**, 673–676 (1979).
 - [2] L. J. Root and J. L. Skinner, *J. Chem. Phys.* **89**, 3279–3284 (1988).
 - [3] P. W. Anderson, *Phys. Rev.* **109**, 1492–1505 (1958).
 - [4] L. S. Levitov, *Europhys. Lett.* **9**, 83 (1989).
 - [5] L. S. Levitov, *Ann. N. Y. Acad. Sci.* **581**, 95–101 (1990).
 - [6] L. S. Levitov, *Phys. Rev. Lett.* **64**, 547–550 (1990).
 - [7] L. S. Levitov, *Ann. Phys. (Leipzig)* **8**, 697–706 (1999).
 - [8] T. Xu and R. V. Krems, *New J. Phys.* **17**, 065014 (2015).
 - [9] J. W. Kantelhardt and A. Bunde, *Ann. Phys. (Leipzig)* **7**, 400–405 (1998).
 - [10] C. A. Müller and D. Delande, *Disorder and interference: localization phenomena in Les Houches 2009 - Session XCI: Ultracold Gases and Quantum Information*, edited by C. Miniatura, L.-C. Kwek, M. Ducloy, B. Gremaud,

- B.-G. Englert, L. Cugliandolo, A. Ekert, K. K. Phua (Oxford University Press, Oxford 2011).
- [11] X. Deng, B. L. Altshuler, G. V. Shlyapnikov, and L. Santos, *Phys. Rev. Lett.* **117** 020401 (2016).
 - [12] A. Frisch, M. Mark, K. Aikawa, S. Baier, R. Grimm, A. Petrov, S. Kotochigova, G. Quémener, M. Lepers, O. Dulieu, and F. Ferlaino, *Phys. Rev. Lett.* **115**, 203201 (2015).
 - [13] K.-K. Ni, S. Ospelkaus, M. H. G. de Miranda, A. Pe'er, B. Neyenhuis, J. J. Zirbel, S. Kotochigova, P. S. Julienne, D. S. Jin, and J. Ye, *Science* **322**, 231 (2008).
 - [14] M. H. G. de Miranda, A. Chotia, B. Neyenhuis, D. Wang, G. Quémener, S. Ospelkaus, J. L. Bohn, J. Ye, and D. S. Jin, *Nat. Phys.* **7** 502 (2011).
 - [15] A. Chotia, B. Neyenhuis, S. A. Moses, B. Yan, J. P. Covey, M. Foss-Feig, A. M. Rey, D. S. Jin, and J. Ye, *Phys. Rev. Lett.* **108** 080405 (2012).
 - [16] B. Yan, S. A. Moses, B. Gadway, J. P. Covey, K. R. A. Hazzard, A. M. Rey, D. S. Jin and J. Ye, *Nature* **501**, 521 (2013).
 - [17] D. Clément, A. F. Varón, J. A. Retter, L. Sanchez-Palencia, A. Aspect, and P. Bouyer, *New J. Phys.* **8**, 165 (2006).
 - [18] J. Billy, V. Josse, Z. Zuo, A. Bernard, B. Hambrecht, P. Lugan, D. Clément, L. Sanchez-Palencia, P. Bouyer, and A. Aspect, *Nature* **453**, 891 (2008).
 - [19] L. Fallani, J. E. Lye, V. Guarrera, C. Fort, and M. Inguscio, *Phys. Rev. Lett.* **98**, 130404 (2007).
 - [20] G. Roati, C. D'Errico, L. Fallani, M. Fattori, C. Fort, M. Zaccanti, G. Modugno, M. Modugno, and M. Inguscio, *Nature* **453**, 895 (2008).
 - [21] D. E. Logan and P. G. Wolynes, *J. Chem. Phys.* **87**, 7199 (1987).
 - [22] Y. Liang, Z. Xu, J. Xia, S.-T. Tsai, Y. Wu, G. Li, C. Ray, and L. Yu, *Adv. Mater.* **22**, E135-E138 (2010).
 - [23] S. H. Park, A. Roy, S. Beaupré, S. Cho, N. Coates, J. S. Moon, D. Moses, M. Leclerc, K. Lee, and A. J. Heeger, *Nat. Photon.* **3**, 297-302 (2009).
 - [24] N. Y. Yao, C. R. Laumann, S. Gopalakrishnan, M. Knap, M. Müller, E. A. Demler, and M. D. Lukin, *Phys. Rev. Lett.* **113**, 243002 (2014).